NONLINEAR FILTERING OF 3D MRI AS APPLICATION OF ŁA$_{\text{sqrt}}$

J. Kukal[1,2]*, D. Majerová*[2]*, A. Procházka*[1] *and J. Šprindrich*[3]

[1] Institute of Chemical Technology, Prague
[2] Czech Technical University in Prague
[3] Charles University in Prague

Abstract

The 3D image of human head obtained by T2 magnetic resonance imaging (MRI) can be represented by three-dimensional matrix of voxel intensities. There is a chance to use eight neighbor voxels for the 3D interpolation. The trivial linear interpolation can be realized as mean of eight. The main disadvantage of linear filtering is a sensitivity to impulse noise. There is a chance to build a set of non-linear filters using Łukasiewicz algebra with square root (ŁA$_{\text{sqrt}}$). They can be both insensitive to impulse noise and similar to linear filters in the case of Gaussian noise. The ŁA$_{\text{sqrt}}$ is a good tool for realization of several trimmed averages, median, quasimedians, L-estimates with dyadic weights, Walsh list, Hodges-Lehmann median and the other useful procedures for non-linear processing. The amazing properties of Hodges-Lehmann are demonstrated on HL$_4$ function. The non-linear functions are used for direct and hierarchical fuzzy denoising. The software for the 3D non-linear denoising of MRI signal was built in the Matlab environment. The filter properties were also studied and compared. Both the statistical analysis of robust filters and the application of them to real biomedical data come to the filters with Walsh list inside. They are robust to impulse noise and similar to the "average of eight" filter.

1 Primer of ŁA$_{\text{sqrt}}$

The mathematical background of 3D image processing is *Łukasiewicz algebra enriched by a square root function* (ŁA$_{\text{sqrt}}$) which is defined as

$$\text{ŁA}_{\text{sqrt}} = \{\mathbf{L}, \wedge, \vee, \otimes, \rightarrow, \text{sqrt}, 0, 1\}$$

where $\mathbf{L} = [0,1] \subset \mathbf{R}$, conjunction ($\wedge$), disjunction ($\vee$), Łukasiewicz multiplication ($\otimes$) and residuum ($\rightarrow$) are basic operations and sqrt is the square root function (Tab. 1). It is useful to introduce several derived operators, e.g. negation, equivalence, non-equivalence, addition or subtraction. We can describe the basic and derived operators as *basic functions* (Tab. 1).

The *fuzzy logic expression* (FLE) is defined by the rules:

- Any free variable $x \in \mathbf{L}$ is FLE.
- Any constant $a \in \mathbf{L}$ is FLE.
- $\psi_i(\text{FLE})$ is FLE for $i = 1, 2$,
- $\psi_j(\text{FLE}, \text{FLE})$ is FLE for $j = 3, \ldots, 10$,
- $\psi_k(\text{FLE}, n)$ is FLE for $k = 11, 12$ and $n \in \mathbf{N}_0$,

  where ψ_m $(m = 1, \ldots, 12)$ are the basic functions in ŁA$_{\text{sqrt}}$.

Let $n \in \mathbf{N}$, $\vec{x} \in \mathbf{L}^n$ and $\varphi : \mathbf{L}^n \rightarrow \mathbf{L}$. If $\varphi(\vec{x})$ is FLE then φ is called a *fuzzy logic function* (FLF) in ŁA$_{\text{sqrt}}$. The main advantage of ŁA$_{\text{sqrt}}$ is a constrain sensitivity of any FLF to its input variables as proven in [3].

function	**formula**
negation	$\psi_1(x) = \neg x = 1 - x$
square root	$\psi_2(x) = \mathrm{sqrt}(x) = (1 + x)/2$
conjunction	$\psi_3(x, y) = x \wedge y = \min(x, y)$
disjunction	$\psi_4(x, y) = x \vee y = \max(x, y)$
Łukasiewicz multiplication	$\psi_5(x, y) = x \otimes y = \max(x + y - 1, 0)$
residuum	$\psi_6(x, y) = x \to y = \min(1 - x + y, 1)$
equivalence	$\psi_7(x, y) = x \leftrightarrow y = 1 - \lvert x - y \rvert$
non-equivalence	$\psi_8(x, y) = x \circ y = \lvert x - y \rvert$
addition	$\psi_9(x, y) = x \oplus y = \min(x + y, 1)$
subtraction	$\psi_{10}(x, y) = x \ominus y = \max(x - y, 0)$
multiplication by integer	$\psi_{11}(x, n) = n \odot x = \min(n \cdot x, 1)$
integer power	$\psi_{12}(x, n) = x^n = \max(n \cdot x - n + 1, 0)$

Table 1: Basic functions in $\mathrm{LA}_{\mathrm{sqrt}}$ for $x, y \in \mathbf{L},\ n \in \mathbf{N}_0$

2 Useful FLFs for 3D Image Denoising

Let $S = (x_1, \ldots, x_n)$ be a list of values $x_k \in [0, 1]$. Let $O = (x_{(1)}, \ldots, x_{(n)})$ be an ordered list of values from S. Let $y \in [0, 1]$ be the output of 3D denoising filter. Then the *FLF denoising filter* is based on the formula

$$y = f(x_1, \ldots, x_n)$$

where $f :\ [0, 1]^n \to [0, 1]$ is a FLF.

It is useful to define *Walsh list* as $n(n + 1)/2$-tuple of FLF

$$W_n : \mathbf{L}^n \to \mathbf{L}^{n(n+1)/2}$$

where

$$\vec{W}_n(\vec{x}) = \left(\frac{x_i + x_j}{2} \;\middle|\; 1 \le i \le j \le n \right).$$

Let $p = \lfloor \frac{n+1}{2} \rfloor$, $q = \lceil \frac{n+1}{2} \rceil$, $r = \lfloor \frac{n}{4} \rfloor$, $s = \frac{n-k}{2}$ and $t = \frac{n-k-1}{2}$. Thus there are several FLFs which can be used for the FLF denoising:

$$\mathrm{AVG}_{n,k}(\vec{x}) = \frac{1}{k} \cdot \sum_{j=1}^{k} x_{(s+j)} \quad \text{for } k = 2^N,$$

$$\mathrm{MED}_{n,k}(\vec{x}) = \frac{1}{2} \cdot \left(x_{(p-k)} + x_{(q+k)} \right) \quad \text{for } k < p,$$

$$\mathrm{BIN}_{n,k}(\vec{x}) = \frac{1}{2^k} \cdot \sum_{j=0}^{k} \binom{k}{j} \cdot x_{(t+j)} \quad \text{for } t \in \mathbf{N},$$

$$\mathrm{BES}_n(\vec{x}) = \frac{1}{2} \cdot \left(\mathrm{MED}_{n,0}(\vec{x}) + \mathrm{MED}_{n,r}(\vec{x}) \right),$$

$$\mathrm{HL}_n(\vec{x}) = \mathrm{MED}_{n(n+1)/2,0}(\vec{W}_n(\vec{x})),$$

$$\mathrm{WBES}_n(\vec{x}) = \mathrm{BES}_{n(n+1)/2}(\vec{W}_n(\vec{x})).$$

They are realizable in $\mathrm{LA}_{\mathrm{sqrt}}$ because of (see [3])

- any $x_{(k)}$ is FLF of $\vec{x} \in \mathbf{L}^n$,

- any weighted sum $\sum_{k=1}^{n} w_k x_k$ is FLF of $\vec{x} \in \mathbf{L}^n$ just when $\sum_{k=1}^{n} w_k \le 1$ and w_k is non-negative dyadic number ($w_k = m_k/2^N$).

There are two extreme approaches to FLF denoising: average making and median making. They are represented by $\mathrm{AVG}_{n,n}$ and $\mathrm{MED}_{n,0}$ functions. The arithmetic mean is too sensitive to impulse noise while the median is robust in this case. But the argumentation against median is based on its inadequate response to Gaussian noise. That is why the compromise processing plays the important role in applications. The Walsh list is an efficient tool for the compromise making.

Example: Let $n = 4$ and $\vec{x} = (x_1, x_2, x_3, x_4)$. Then there are only four different FLF filters: $\mathrm{AVG}_{4,4}$, $\mathrm{MED}_{4,0}$, $\mathrm{BIN}_{4,3}$ and HL_4. In the trivial case $x_1 = x_2 = x_3 = x_4 = \xi$, we have $\mathrm{AVG}_{4,4}(\vec{x}) = \mathrm{MED}_{4,0}(\vec{x}) = \mathrm{BIN}_{4,3}(\vec{x}) = \mathrm{HL}_4(\vec{x}) = \xi$. Otherwise, the vector $\vec{x} \in \mathbf{L}^4$ can be normalized and permuted to the form $\vec{x} = (a, b, 0, 1)$ where $a, b \in \mathbf{L}$. Then $x_{(1)} = 0$, $x_{(2)} = \min(a, b)$, $x_{(3)} = \max(a, b)$, $x_{(4)} = 1$ and finally $\mathrm{AVG}_{4,4}(\vec{x}) = (a+b+1)/4$, $\mathrm{MED}_{4,0}(\vec{x}) = (a+b)/2$, $\mathrm{BIN}_{4,3}(\vec{x}) = (3a + 3b + 1)/8$, $\vec{W}_4(\vec{x}) = (a, (a + b)/2, a/2, (a + 1)/2, b, b/2, (b + 1)/2, 0, 1/2, 1)$, $\mathrm{HL}_4(\vec{x}) = \mathrm{MED}_{10,0}(\vec{W}_4(\vec{x}))$. It is easy to demonstrate that the values $\mathrm{BIN}_{4,3}(\vec{x})$ and $\mathrm{HL}_4(\vec{x})$ are between $\mathrm{AVG}_{4,4}(\vec{x})$ and $\mathrm{MED}_{4,0}(\vec{x})$.

The contour plot of $\mathrm{AVG}_{4,4}(a, b, 0, 1)$ is depicted in the Fig. 2 for the contour distance $\Delta\mathrm{FLF} = 0.01$. The contour plots of $\mathrm{MED}_{4,0}(a, b, 0, 1)$, $\mathrm{BIN}_{4,3}(a, b, 0, 1)$ and $\mathrm{HL}_4(a, b, 0, 1)$ are depicted in the Figs. 3–5.

The $\mathrm{BIN}_{4,3}(\vec{x})$ is a trivial compromise between mean and median because of $\mathrm{BIN}_{4,3}(\vec{x}) = (\mathrm{AVG}_{4,4}(\vec{x}) + \mathrm{MED}_{4,0}(\vec{x}))/2$. The Hodges-Lehmann median (see [2]) $\mathrm{HL}_4(a, b, 0, 1)$ offers the same value as $\mathrm{AVG}_{4,4}(a, b, 0, 1)$ for $\min(a, b) \le 1/2 \le \max(a, b)$. The value $\mathrm{HL}_4(a, a, 0, 1) = a$ is equal to the median $\mathrm{MED}_{4,0}(a, a, 0, 1) = a$. Then the $\mathrm{HL}_4(\vec{x})$ function based on Walsh list $\vec{W}_4(\vec{x})$ is robust to impulse noise as median but near to the mean for the symmetric values which is useful for image denoising.

3 Direct FLF Denoising

Let the values $x_1, \ldots, x_8$ are obtained from the $2 \times 2 \times 2$ cube of eight neighbor voxels from the original 3D image. The direct FLF denoising is a process of the "body centered" interpolation which is not necessary linear one. We can use any FLF and apply it to the original corner values $x_1, \ldots, x_8$.

The functions $\mathrm{AVG}_{8,8}$, $\mathrm{AVG}_{8,4}$, BES_8, $\mathrm{MED}_{8,0}$, $\mathrm{MED}_{8,1}$, HL_8, WBES_8, $\mathrm{BIN}_{8,3}$, $\mathrm{BIN}_{8,5}$, $\mathrm{BIN}_{8,7}$ were used for the direct FLF denoising.

4 Hierarchical FLF Denoising

The 2^3 cube of eight voxels can be decomposed in three directions to the three pairs of 2^2 squares. Then the six lists of size four are formed

$$\begin{aligned} S_1 &= (x_1, x_2, x_3, x_4) \\ S_2 &= (x_5, x_6, x_7, x_8) \\ S_3 &= (x_1, x_2, x_5, x_6) \\ S_4 &= (x_3, x_4, x_7, x_8) \\ S_5 &= (x_1, x_3, x_5, x_7) \\ S_6 &= (x_2, x_4, x_6, x_8) \end{aligned}$$

The first step of hierarchical FLF processing is based on the "face centered" interpolation using any FLF. The functions $\mathrm{MED}_{4,0}$, HL_4 were used here to produce $h_k = f(S_k)$ for $k = 1, \ldots, 6$.

The second and last step is based on the denoising by the six points interpolation using the another FLF. The functions $\mathrm{AVG}_{6,4}$, $\mathrm{MED}_{6,0}$ and HL_6 were used to obtain $y = f(h_1, \ldots, h_6)$.

5 Filter Testing

A set of sixteen FLF 3D filters was tested using the impulse and Gaussian noise. The impulse noise was represented by a list where $x_1 = 1$ and $x_k = 0$ for $k = 2, \ldots, 8$. The Gaussian noise was studied in the case when $x_k \sim N(0.5, 0.01)$ for $k = 1, \ldots, 8$. Then the standard deviation of Gaussian noise is $\sigma = 0.1$. The results are collected in the Tab. 2. Every filter is described by a single FLF or by a pair of two FLFs. The output response to a single impulse noise is denoted as y_I and its ideal value is zero. The experimental values of standard deviation gain s_G/σ are also included in the Tab. 2 for the Gaussian noise and 10^4 samples.

Filter	**1st level**	**2nd level**	y_I	s_G/σ
F_1	$\mathrm{AVG}_{8,8}$	*	0.1250	**0.3554**
F_2	$\mathrm{AVG}_{8,4}$	*	0.0000	0.3858
F_3	BES_8	*	0.0000	0.3688
F_4	$\mathrm{MED}_{8,0}$	*	0.0000	0.4102
F_5	$\mathrm{MED}_{8,1}$	*	0.0000	0.3887
F_6	HL_8	*	0.0000	0.3670
F_7	WBES_8	*	0.0000	**0.3603**
F_8	$\mathrm{BIN}_{8,3}$	*	0.0000	0.3947
F_9	$\mathrm{BIN}_{8,5}$	*	0.0000	0.3853
F_{10}	$\mathrm{BIN}_{8,7}$	*	0.0078	0.3781
F_{11}	$\mathrm{MED}_{4,0}$	$\mathrm{AVG}_{6,4}$	0.0000	0.3806
F_{12}	$\mathrm{MED}_{4,0}$	$\mathrm{MED}_{6,0}$	0.0000	0.3863
F_{13}	$\mathrm{MED}_{4,0}$	HL_6	0.0000	0.3794
F_{14}	HL_4	$\mathrm{AVG}_{6,4}$	0.0000	0.3663
F_{15}	HL_4	$\mathrm{MED}_{6,0}$	0.0000	0.3703
F_{16}	HL_4	HL_6	0.0000	0.3648

Table 2: FLF filter properties

There are only two filters (F_1, F_{10}) which are sensitive to the impulse noise. The other filters are robust ones. The F_1 filter is just linear one with the smallest possible gain $s_G/\sigma = 0.3554$ of Gaussian noise. The best non-linear filter with minimum noise gain $s_G/\sigma = 0.3603$ is F_7 which is represented by WBES_8 FLF. The top five robust filters with zero sensitivity to impulse noise are F_7, F_{16}, F_{14}, F_6, F_3 with $s_G/\sigma \leq 0.37$. The time complexity of FLF filtering is driven by the time complexity of sorting the lists. Supposing the time complexity $\mathrm{T}(n) \approx n(n-1)/2$ of n-element sorting, we obtain the time complexities of the top five filters proportional to 630, 480, 285, 630 and 28.

6 Biomedical Application

The set of FLF filters were applied to 3D MRI T2 image and the results were compared. There is no possibility to compare the resulting 3D images with the ideal 3D image because of it is unknown. That is why the 3D images were compared each to other using euclidean distance

$$d : [0;1]^{m\times n\times p} \times [0;1]^{m\times n\times p} \to \mathbf{R}_0^+$$

in the space $[0;1]^{m\times n\times p}$, where $m, n, p \in \mathbf{N}$ are 3D image dimensions. The distance is defined as

$$d(\mathbf{A}, \mathbf{B}) = \sqrt{\sum_{i=1}^{m}\sum_{j=1}^{n}\sum_{k=1}^{p}(a_{ijk} - b_{ijk})^2}$$

and the mutual distances

$$d_{i,j} = d(\mathbf{F}_i(\mathbf{X}), \mathbf{F}_j(\mathbf{X}))$$

forms the matrix

$$\mathbf{D} = \{d_{i,j}\}_{i,j=1}^{N}$$

where $N \in \mathbf{N}$ is a member of filters, $\mathbf{X} \in [0;1]^{m \times n \times p}$ is the original 3D image and $\mathbf{F}_i(\mathbf{X}) \in [0;1]^{m \times n \times p}$ is the result of i^{th} FLF filter. Using a distance threshold value $\theta > 0$, we can study similar FLF filters satisfying $0 < d_{i,j} \leq \theta$ in the biomedical context. The graph theory enables to show the relationships using undirected graph with FLF filters as vertices and with edges as symbols of filter similarity. The adjacency matrix is then defined as

$$\mathbf{A} = \{a_{ij}\}_{i,j=1}^{N}$$

where $a_{ij} = (d_{i,j} > 0) \wedge (d_{i,j} \leq \theta)$. Applying the methodology to the original 3D image $\mathbf{X}$ (Fig. 6), the sixteen FLF filters (Tab. 2) and the distance threshold $\theta = 7.5$, we have $N = 16$ together with the matrices $\mathbf{D}, \mathbf{A}$. The resulting undirected graph has five components (Fig. 1). The first component consists of eight filters (vertices): F_2, F_4, F_8–F_{13} which are similar to the median filter F_4 ($MED_{8,0}$). There is a maximum clique of size five inside the first component: F_2, F_8, F_9, F_{10}, F_{12}. The second component consists of five filters: F_6, F_7, F_{14}, F_{15}, F_{16} which use Walsh list as a background of FLF processing. There is a unique maximum clique of size three inside the second component: F_7, F_{14}, F_{16}. The remaining three components consist of single isolated filters: F_1, F_3, F_5. The cluster analysis of previous results was also based on the analysis of the distance matrix $\mathbf{D}$. Splitting the filters into two clusters we obtain two classes: F_1, F_3, F_6, F_7, F_{13}–F_{16} and F_2, F_4, F_5, F_8–F_{12}. The first class includes the arithmetic mean $AVG_{8,8}$, BES_8 and the filters with Walsh list inside. The second class consists of the remaining filters which are similar to the median $MED_{8,0}$. Cluster analysis into three clusters forms a new cluster: F_5, F_6, F_{15}. The other clusters are: F_1, F_3, F_7, F_{13}, F_{14}, F_{16} and F_2, F_4, F_8–F_{12}. Cluster analysis into four clusters forms a new cluster: F_3, F_{11}, F_{13}, F_{14}. The other clusters are: F_1, F_7, F_{16} then F_2, F_4, F_8–F_{10}, F_{12} and F_5, F_6, F_{15}. Finally, the splitting into five clusters produces "mean" cluster: F_1, F_7, F_{16}, "median" cluster: F_4, F_8, F_9, F_{12}, "trimmed" cluster: F_2, F_{10}, "BES" cluster: F_3, F_{11}, F_{13}, F_{14} and "Hodges-Lehmann" cluster: F_5, F_6, F_{15}. Here, the "mean" cluster consists of top three filters with $s_G/\sigma \leq 0.365$. Thus the robust filters F_7 ($WBES_8$) and F_{16} ($HL_4 + HL_6$) are recommended as closed to F_1 ($AVG_{8,8}$) on the MRI 3D data. But the "median" cluster consists of filters with $s_G/\sigma \geq 0.385$ which are not recommended to the robust filtering of MRI 3D signal.

7 Conclusions

A class of 16 non-linear 3D FLF filters was developed, analyzed and tested on artificial and biomedical data. There are two representative subclasses of robust FLF filters which are either similar to median or using Walsh list in the first level of FLF processing. The second subclass of 3D FLF filters is recommended for 3D MRI processing because of small gain of Gaussian noise. This result was obtained on real biomedical data using graph theory and cluster analysis as two analytical approaches.

From the biomedical point of view, the highest possible space resolution, the morphological contrast and absence of artefacts are necessary for exact anatomical recognition of displayed structures. The improved filtering of MRI signals is one of important factors within the process of their transformation to the visual form. From that point of view, the result of non-linear 3D denoising plays a role in medical praxis.

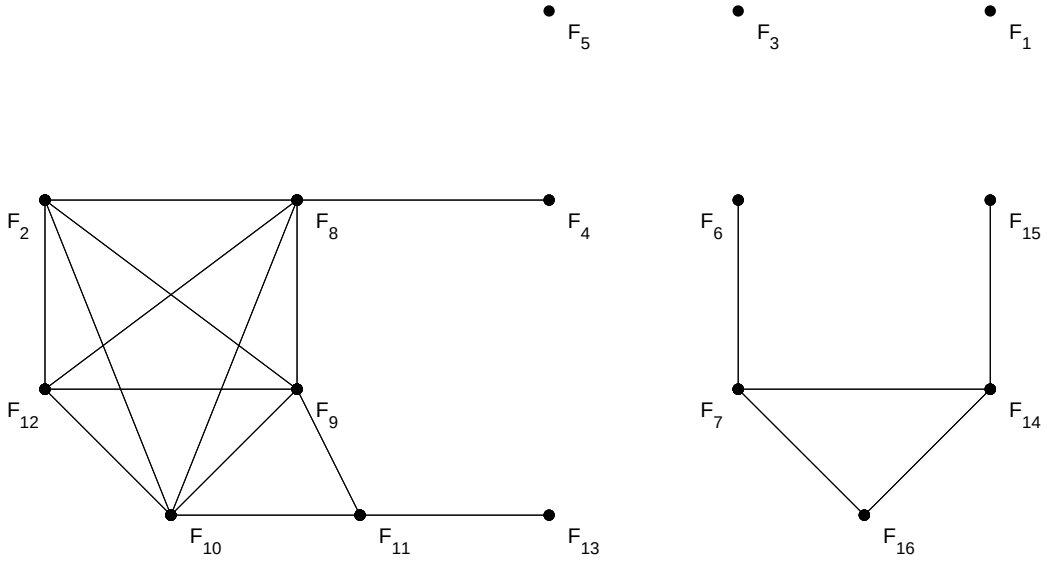

Figure 1: Graph of 3D FLF class

References

[1] Mitra, S. K., Kaiser, J. F.: *Handbook for Digital Signal Processing*. John Wiley & Sons. New York. 1993.

[2] Hodges, J. L., Lehmann, E. L. On Medians and Quasi Medians. *Journal of the American Statistical Association*, 1967, 62, p.926–931.

[3] Majerová, D., Kukal, J. Multicriteria approach to 2D image de-noising by means of Łukasiewicz algebra with square root. *Neural Network World*, 2002, 12, p. 333–348.

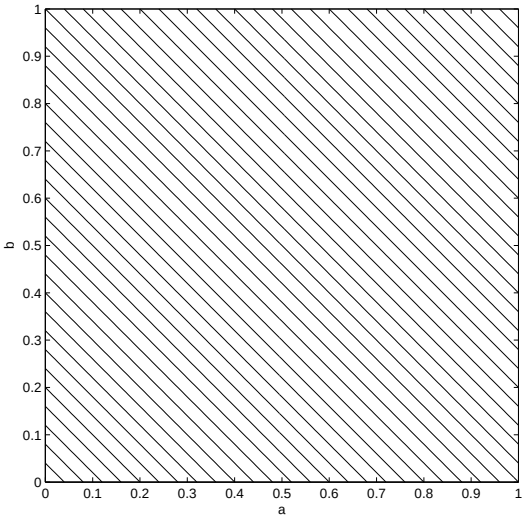

Figure 2: Contour plot of $\mathrm{AVG}_{4,4}(a, b, 0, 1)$

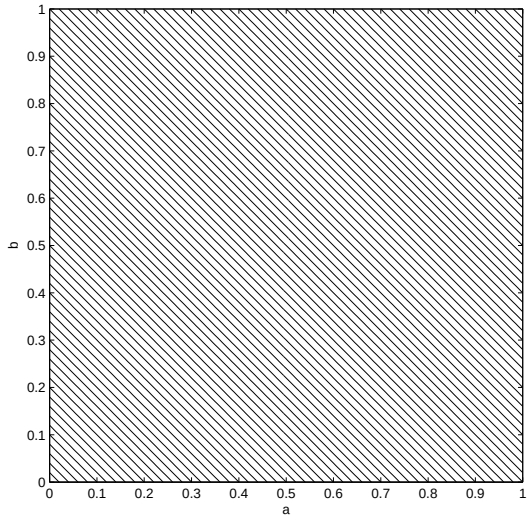

Figure 3: Contour plot of $\mathrm{MED}_{4,0}(a, b, 0, 1)$

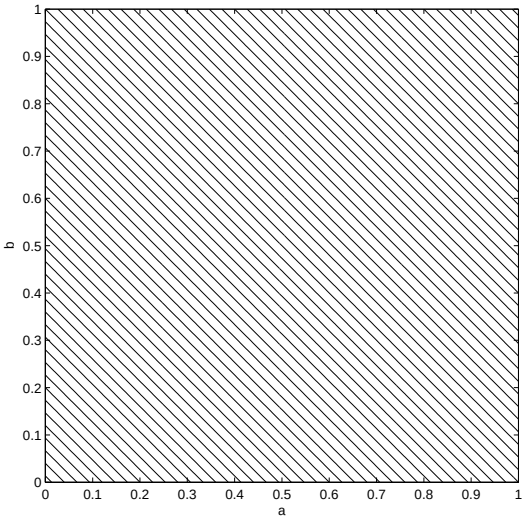

Figure 4: Contour plot of $\mathrm{BIN}_{4,3}(a, b, 0, 1)$

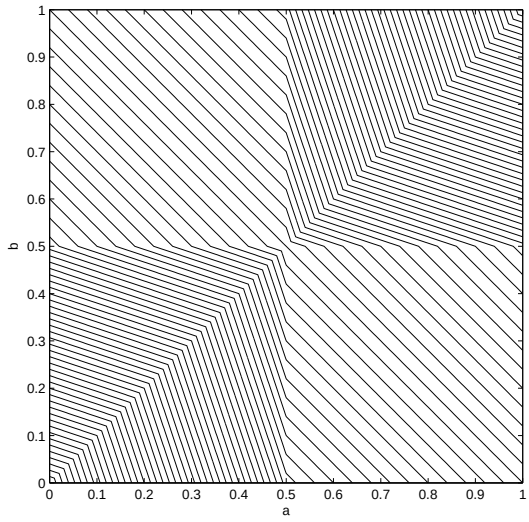

Figure 5: Contour plot of $\mathrm{HL}_4(a, b, 0, 1)$

Figure 6: Original image (slice 90)

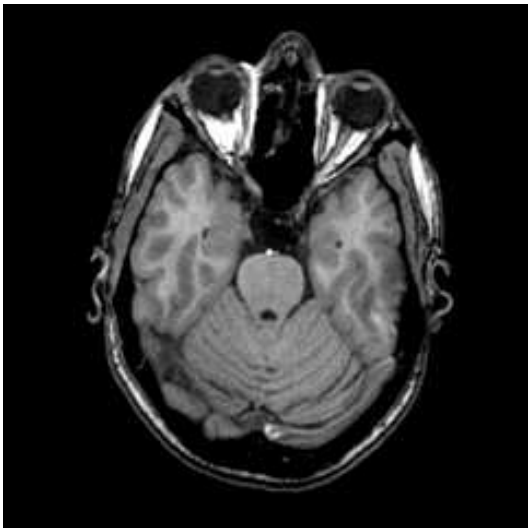

Figure 7: Filter F_1—$\mathrm{AVG}_{8,8}$

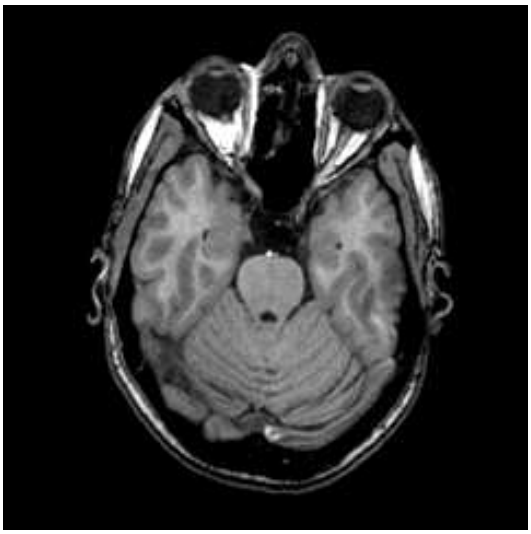

Figure 8: Filter F_7—WBES_8

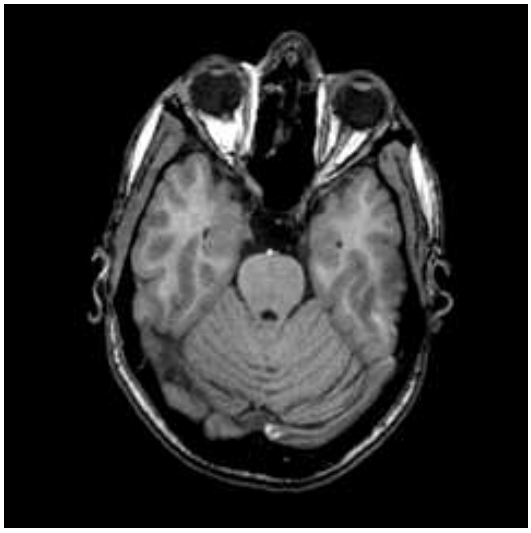

Figure 9: Filter F_{16}—HL_4 before HL_6

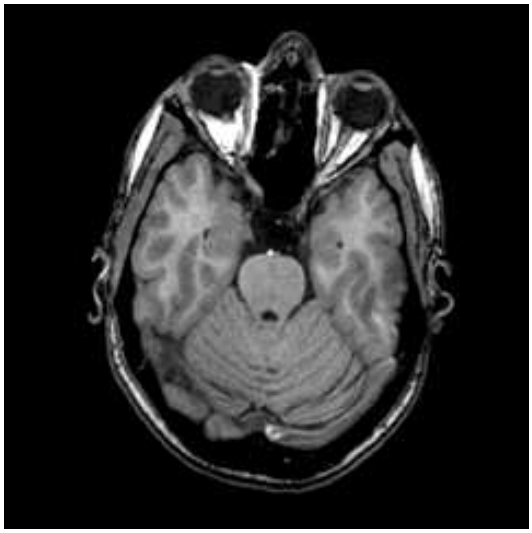

Figure 10: Filter F_{14}—HL_4 before $AVG_{6,4}$

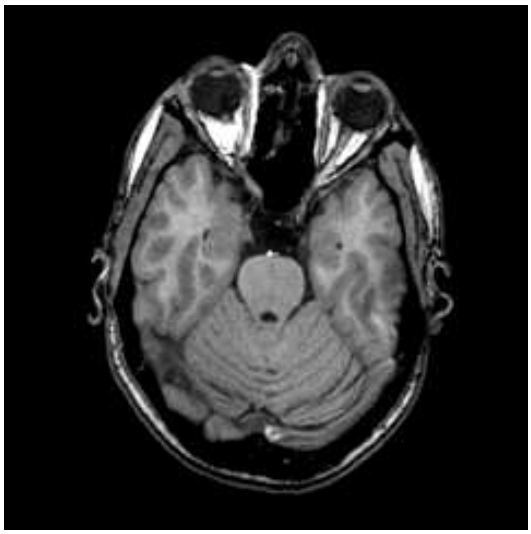

Figure 11: Filter F_6—HL_8

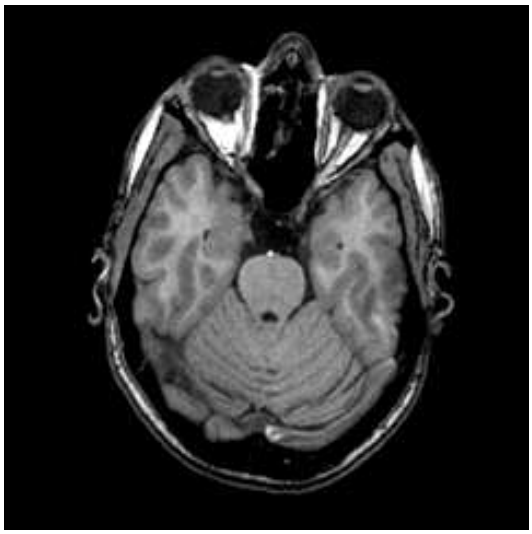

Figure 12: Filter F_3—BES_8

Jaromír Kukal
[1] Institute of Chemical Technology, Prague
Faculty of Chemical Engineering
Department of Computing and Control Engineering
Technická 5, 166 28 Prague 6 – Dejvice
[2] Czech Technical University in Prague
Faculty of Nuclear Sciences and Physical Engineering
Department of Software Engineering in Economy
Trojanova 13, 120 00 Prague 2
Phone: +420 224 358 583
E-mail: Jaromir.Kukal@dc.fjfi.cvut.cz

Dana Majerová
Czech Technical University in Prague
Faculty of Nuclear Sciences and Physical Engineering
Department of Software Engineering in Economy
Pohraniční 1288/1, 405 01 Děčín 1
Phone: +420 224 358 481, fax: +420 412 512 730
E-mail: Dana.Majerova@dc.fjfi.cvut.cz

Aleš Procházka
Institute of Chemical Technology, Prague
Faculty of Chemical Engineering
Department of Computing and Control Engineering
Technická 5, 166 28 Prague 6 – Dejvice
Phone: +420 224 354 170, fax: +420 224 355 053
E-mail: A.Prochazka@ieee.org
WWW address: http://dsp.vscht.cz/

Jan Šprindrich
Charles University Prague
3rd Faculty of Medicine
Clinic of Diagnostic Radiology
Šrobárova 50, 100 34 Prague 10
Phone: +420 296 472 812
E-mail: Sprind@fnkv.cz